Prototropism of [2,2'-Bipyridyl]-3,3'-diol in Albumin-SDS Aggregates

ARTICLE *in* THE JOURNAL OF PHYSICAL CHEMISTRY B · AUGUST 2012

Impact Factor: 3.3 · DOI: 10.1021/jp306027h · Source: PubMed

3 AUTHORS:

Dipanwita De
Indian Institute of Technology Bombay
3 PUBLICATIONS **27** CITATIONS
SEE PROFILE

Kalyan Santra
Indian Institute of Technology Bombay
1 PUBLICATION **9** CITATIONS
SEE PROFILE

Anindya Datta
Indian Institute of Technology Bombay
86 PUBLICATIONS **2,084** CITATIONS
SEE PROFILE

Available online at www.sciencedirect.com
ScienceDirect
Chemical Physics Letters 438 (2007) 218–223
CHEMICAL PHYSICS LETTERS
www.elsevier.com/locate/cplett

2-(2′-Pyridyl)benzimidazole as a fluorescent probe for monitoring protein–surfactant interaction

Tushar Kanti Mukherjee, Priyanka Lahiri, Anindya Datta *

Department of Chemistry, Indian Institute of Technology Bombay, Powai, Mumbai 400 076, India

Received 11 December 2006; in final form 21 February 2007
Available online 12 March 2007

Abstract

The effectiveness of 2-(2′-pyridyl)benzimidazole (2PBI) as a fluorescent probe of macromolecular interactions is investigated, with the well-known human serum albumin–sodium dodecyl sulfate aggregates as the test system. The second fluorescence band of 2PBI, arising from a proton-transferred state at the surface of negatively charged sodium dodecyl sulfate micelles, is suppressed in the aggregates. The temporal features reflect the change in the relative population of the cationic and normal forms of the fluorophore. Thus, 2PBI is found to be a potentially good fluorophore for the study of complex systems like protein–surfactant aggregates.

1. Introduction

2-(2′-Pyridyl)benzimidazole (2PBI) undergoes a solvent-mediated excited-state proton transfer (ESPT) in its cationic form, manifested in a fluorescence band at 455 nm, which grows in time at the cost of the normal emission at 380 nm (Scheme 1) [1]. Recently, we have demonstrated that the ESPT can occur at negatively charged interfaces between water and apolar pseudophases of microheterogeneous media, by virtue of a lower local pH as well as a shift in the pK_a of 2PBI [2–4]. With this background, we now explore if the fluorophore can mark complex phenomena like macromolecular interaction involving negative surfactants, where the structure of the charged interface is disrupted. If the tautomer emission is hindered consequently, then this provides a simple fluorescence ratiometric pointer for macromolecular interactions. In order to test this hypothesis, we have chosen to explore the well-known SDS–albumin interactions brief account of which is provided below [5–15].

Surfactants, at very low concentrations, bind specifically at the high-energy binding sites in the protein, causing an increase in the apparent critical micellar concentration (CMC). Denaturation occurs beyond their critical association concentrations (CAC) due to co-operative binding [8,16]. The interaction is commonly described by the necklace and bead model, in which the proteins wrap around surfactant molecules (Scheme 2) [8,17]. Two homologous albumins have been used in the present study. Despite their structural similarity, they interact differently with ionic surfactants [15,18]. In the present paper, we attempt to understand if 2PBI can serve as an extrinsic fluorescent probe that can be used to differentiate between the interactions of the two albumins with SDS.

2. Experimental

2-(2′-Pyridyl)benzimidazole (AR grade), sodium dodecyl sulfate (SDS) and human serum albumin (HSA) from Aldrich and Bovine Serum Albumin (BSA) (fraction V) from Merck are used as received. 10 μM 2PBI and 0–10 μM proteins are used. The pH of doubly distilled water solutions is 7.2. Absorption and fluorescence spectra are recorded on a JASCO V530 spectrophotometer with a 2 nm band-pass and a Perkin–Elmer LS-55 spectrofluorimeter with $\lambda_{ex} = 310$ nm, respectively. Fluorescence decays are recorded at a magic angle of 54.7° on an Edinburgh

* Corresponding author. Fax: +91 22 2572 34.
E-mail address: anindya@chem.iitb.ac.in (A. Datta).

0009-2614/$ - see front matter © 2007 Elsevier B.V. All rights reserved.
doi:10.1016/j.cplett.2007.03.014

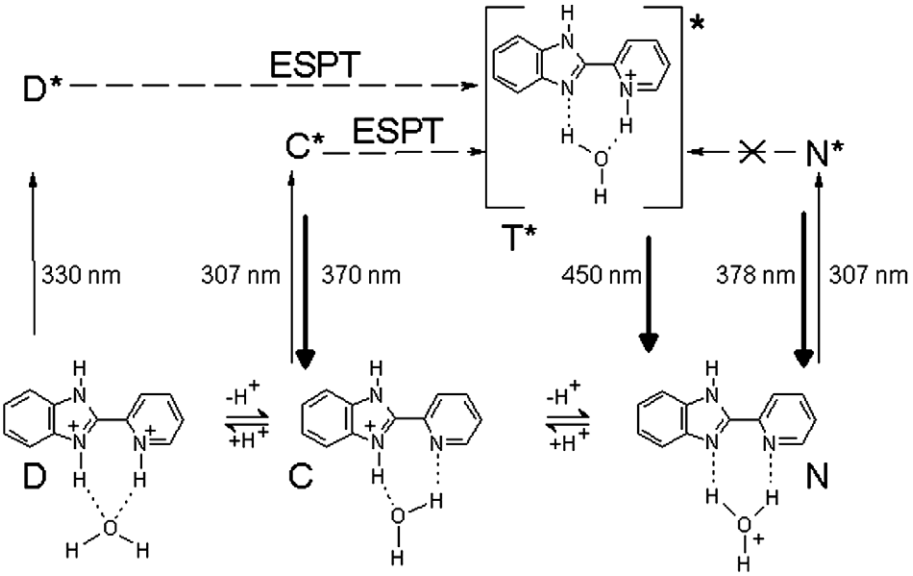

Scheme 1. The species and processess involved in the ESPT of 2PBI.The thin solid arrows denote the absorption process. The dashed and thick solid lines denote nonradiative and radiative transitions, respectively The numbers adjacent to the arrows denote the wavelengths of the absorption/emission maxima.

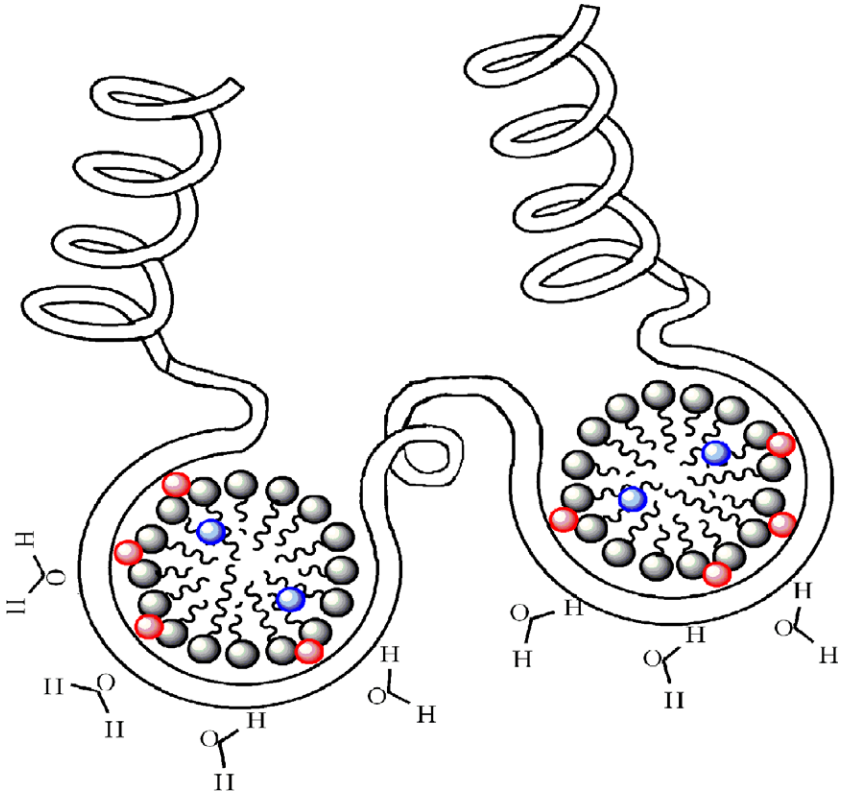

Scheme 2. The necklace and bead model of protein–surfactant interaction. The red and blue circle denotes the cationic and neutral form of 2PBI respectively. (For interpretation of the references in colour in this Scheme, the reader is referred to the web version of this article.)

TCSPC spectrometer, with $\lambda_{ex} = 307$ nm, obtained from the third harmonic of a mode-locked Ti:sapphire laser from Coherent Inc., Palo Alto, CA [19]. They are fitted to single or biexponential functions after deconvolution of the instrument response function (IRF) by the iterative reconvolution method using IBH DAS 6.0 software.

3. Results and discussion

The unaltered absorption and fluorescence spectra of 2PBI upon addition of BSA and HSA, indicate that the fluorophore does not bind with these proteins as such. Upon gradual addition of the proteins to a solution of 2PBI containing 20 mM SDS, its absorption band becomes broadened and red shifted (Fig. 1), indicating the incorporation of the fluorophore in the protein–surfactant complex. Changes in the fluorescence spectra are more remrkable. The tautomer band at 455 nm, which is as strong as the normal band at 365 nm, depletes while the normal band gets shifts to 383 nm in presence of 1×10^{-5} M BSA and 1×10^{-6} M HSA, with concomitant increase in the fluorescence quantum yield (Fig. 1). Isoemissive points (354 nm 428 nm for BSA, 362 and 422 nm for HSA) indicates the equilibria among different forms of the fluorophore.

The red shift and enhanced fluorescence in the normal emission band and the depletion of the tautomer emission mark the disruption of the negatively charged interface between the aqueous and nonpolar pseudophases [2–4]. A significant difference between the extents of interaction with BSA and HSA is indicated in the vanishing of the tautomer emission at 10 μM BSA, but at 1 μM HSA. This clearly indicates that the extent of aggregation of SDS is greater in case of HSA compared to that of BSA, which is in agreement with an earlier report [20]. This is because strong electrostatic as well as hydrophobic interactions govern the SDS–BSA interaction, whereas hydrophobic interactions predominantly govern the HSA–SDS interaction [15,18].

We have resolved the fluorescence spectra as a sum of two Gaussian functions which represent the normal (N*) and the tautomer emissions The normal emission spectra thus obtained (S) have been further expressed as the linear sum of the spectra originating from the fluorophores bound to the protein–surfactant complexes (S_1) and those bound to free micelles (S_2). S_1 and S_2 have been assumed

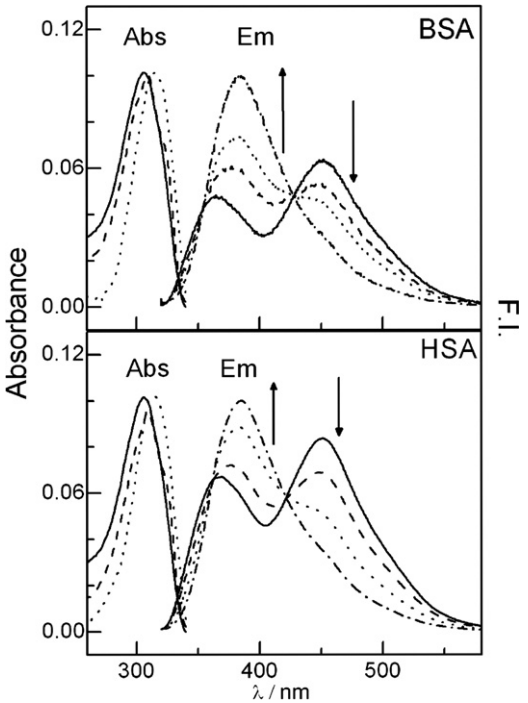

Fig. 1. Absorption (Abs) and fluorescence (Em) spectra of 2PBI in aqueous solutions containing surfactant–protein mixtures. Absorption spectra in upper panel: 10 μM BSA (——), 20 mM SDS (---) and their mixture (·····). Lower panel: 1 μM HSA (——), 20 mM SDS (---) and their mixture (·····). The fluorescence spectra are in 20 mM SDS, with increasing concentrations of the proteins in the direction of the arrows. Upper panel: Spectra at BSA concentrations of 0 (——), 4 (---), 6 (·····) and 10 (-·-·-·-·)μM. Lower panel:spectra at HSA concentrations of 0 (——), 0.4 (---), 0.8 (·····) and 1 (-·-·-·)μM.

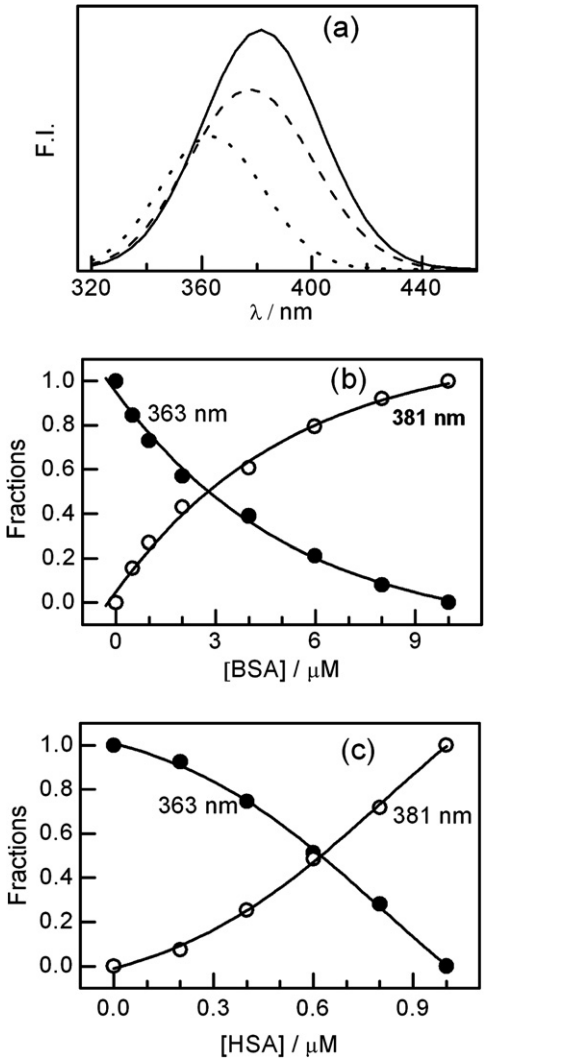

Fig. 2. (a) The normal component of the emission spectra (dashed line) of 2PBI in 20 mM SDS and 6 μM BSA, expressed as a weighted sum of the spectra in 20 mM SDS ($\lambda_{max} = 363$ nm, dotted line) and in 20 mM SDS in presence of 10 μM BSA ($\lambda_{max} = 381$ nm, solid line). The normal components in the presence of constant concentration of the SDS and varying concentrations of proteins are expressed as similar sums and the fractional population of the two components (363 nm and 381 nm), in 20 mM SDS solution, with gradual addition of BSA and HSA are shown in panels (b) and (c) respectively.

to identical to the normal emission spectrum in the presence of 20 mM SDS, in the absence and presence of highest concentrations of the proteins (10 μM in case of BSA and 1 μM in case of HSA) respectively. The plot of the contributions of the two components against protein concentration (Fig. 2) reveals that 2PBI molecules are progressively removed from the water–surfactant interface, but at higher concentrations of BSA compared to HSA.

The protein–surfactant interaction is manifested in an increase in the apparent critical micellar concentration (CMC) of surfactants in the presence of the macromolecule, the extent of which depends on the protein concentration and the extent of the binding of the surfactants with it [20]. In order to explore the ability of 2PBI to act as a reporter fluorophore for this phenomenon, SDS has been added gradually to 2PBI solutions containing fixed concentrations of the proteins. The changes in fluorescence quantum yield are qualitatively similar to our earlier observation in SDS micelles in the absence of proteins [2], but the changes occur at much higher concentrations of SDS due to the protein-induced increase in apparent CMC (Figs. 3 and 4). The initial increase (24 mM to 50 mM SDS) in quantum yield of 380 nm band is due to the hydrophobic character of the protein–surfactant complex. Subsequently, the single emission band at 380 nm indicates that the added surfactant molecules exclusively go into the protein-surfactant complex, with no free micelle below 50 mM SDS. [8,10]. Then, the tautomer band becomes prominent, indicating the formation of free micelles. The peak position and quantum yield saturate at 200 mM SDS, with the normal peak at 365 nm, comparable with that in free SDS

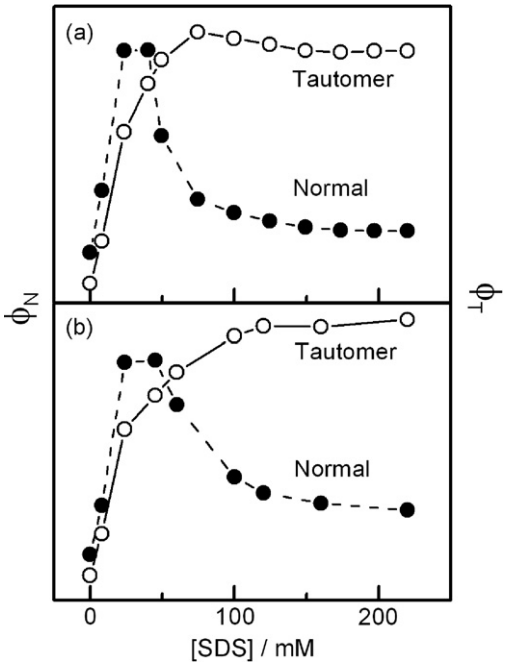

Fig. 3. Variation of relative quantum yields of normal and tautomer emissions of 2PBI with SDS concentration in (a) 1×10^{-5} M BSA and (b) 1×10^{-5} M HSA.

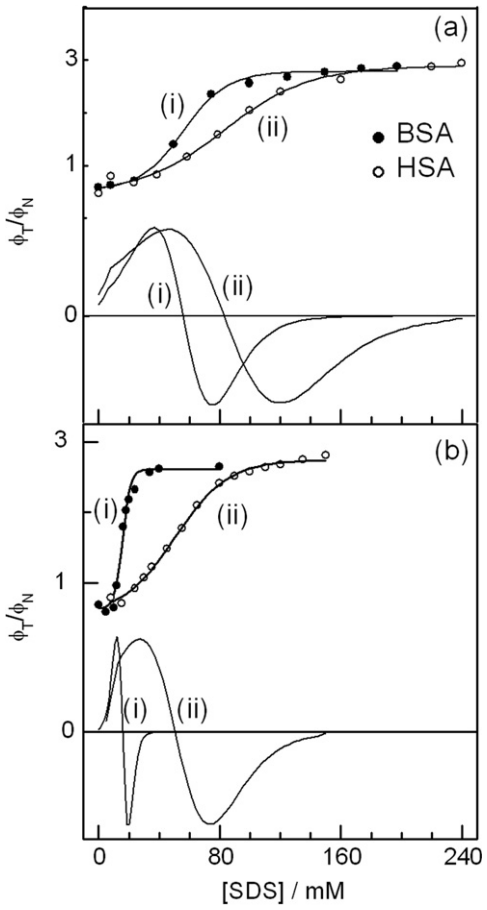

Fig. 4. Variation of the ratio of relative quantum yields of the tautomer and normal species and the double derivative plots of the fitted function as a function of SDS concentration in the presence of (a) 10 μM protein concentration (i) BSA, (ii) HSA and (b) 5 μM protein concentration (i) BSA, (ii) HSA.

micelles. Similar results are obtained on addition of SDS into 1×10^{-5} M solution of HSA. However the tautomer emission becomes prominent at 60 mM SDS. The peak position and quantum yields of both bands saturate at 220 mM with the normal peak appearing at 367 nm.

The variation of the ratio of relative quantum yield of tautomer and normal form with the SDS concentration is a good marker of the apparent CMC of SDS in presence of BSA and HSA (Fig. 4). The point of inflection of the sigmoidal curve determined from the second derivative of the fitted function has a value of 56 mM in case of 1×10^{-5} M BSA and 81 mM in case of 1×10^{-5} M HSA (Fig. 4a). The CMC of SDS is found to depend on the protein concentration. At a protein concentration of 0.5×10^{-5} M BSA and 0.5×10^{-5} M HSA the respective CMCs are 15 mM and 50 mM (Fig. 4b). Thus, we find that the extent of association of SDS is higher with HSA as compared to BSA as the saturation binding point of SDS is higher in case of HSA compared to BSA. Besides, 2PBI is found to correctly report the concentration dependence of the apparent CMC of the surfactant.

Table 1
Fluorescence decay parameters of 2PBI in 20 mM SDS upon addition of proteins at 380 nm

(BSA)/μM	τ_1/ns	τ_2/ns	a_1	a_2	χ^2
0	0.35	0.77	0.33	0.67	1.12
2	0.32	1.30	0.52	0.48	1.16
3	0.33	1.46	0.47	0.53	1.18
5	0.28	1.58	0.38	0.62	1.17
6	0.24	1.63	0.37	0.63	1.14
10	0.21	1.78	0.42	0.58	1.11
(HSA)/μM					
0	0.38	0.72	0.30	0.70	1.01
0.2	0.43	1.03	0.50	0.50	1.02
0.3	0.42	1.17	0.49	0.51	1.17
0.5	0.44	1.29	0.51	0.49	1.11
0.8	0.40	1.33	0.46	0.54	1.15
1.0	0.40	1.32	0.45	0.55	1.15

The fluorescence decay of 2PBI in 20 mM SDS is biexponential, the time constants are 0.35 ns (35%) and 0.80 ns (65%) (Table 1), assigned to the normal (N*) and the cationic (C*) forms, respectively [1,2]. The significantly larger contribution of C* emission in the micelle, compared to the 10% in aqueous solutions [1] is explained by altered pK_a as well as lower local pH [21,22,23, supplementary information] at the Stern layer, where the cation is expected to reside, due to the favorable electrostatic attraction. The first addition of BSA (2 μM) leaves the normal lifetime unchanged, but causes an increase in its fractional contribution from 0.33 to 0.52. The lifetime of C* increases almost twofold (Fig. S2, Table 1), even as its contribution decreases, proportional to the increase in the contribution of the N* emission. Qualitatively similar changes occur upon addition of 0.2 μM HSA. This corroborates with the model of protein–surfactant interaction (Scheme 2). The sharp increase in the contribution of N* in the fluorescence decays, upon addition of the proteins is an evidence of sequestering of the surfactants from the water molecules through formation of the aggregates, thereby leading to a greater concentration of the normal form. The increase in lifetime of the cationic form, on the other hand, can be attributed to a more hydrophobic environment in the aggregates, as well as a decrease in the extent of the nonradiative ESPT process due to the exclusion of water which is an essential component required to bring about the process at negatively charged interfaces (Scheme 1) [2–4]. On subsequent addition of proteins, the lifetime as well as the contribution of C* increase (Table 1). Previously it has been shown that the microenvironment of the protein–surfactant aggregates is less polar compared to that of free micelles due to the lower availability of water molecules [24]. Additionally, an explanation can be provided in the light of the interaction of the unsolvated negatively charged headgroups of SDS with the cationic form, which can stabilize it in the ground state to a greater extent than solvated headgroups, leading to an increase in the ground state contribution of the cation compared to the normal form.

The discussion presented above gains further support from the experiment where the concentration of the proteins are kept constant and SDS is added gradually. Upon the first addition of SDS, the 60 ps component in water, ascribed to N*, increases to 130 ps in case of BSA and 80 ps in case of HSA (Fig. 5, Table 2). This increase in life-

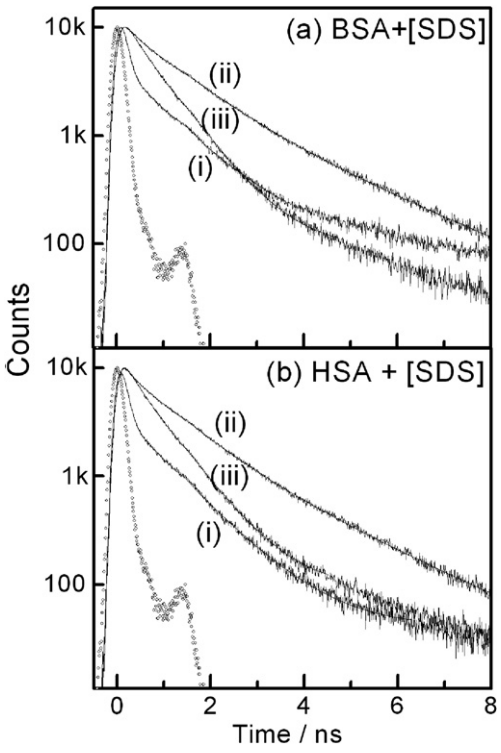

Fig. 5. Fluorescence decays of 2PBI in (a) 10 μM BSA and (b) 10 μM HSA with (i) 0 mM, (ii) 24 mM, (iii) 200 mM SDS at 380 nm.

Table 2
Fluorescence decay parameters of 2PBI in 10 μM of proteins upon addition of SDS at 380 nm

BSA + (SDS)/mM	τ_1/ns	τ_2/ns	a_1	a_2	χ^2
0	0.06	1.00	0.91	0.09	0.95
8	0.13	1.29	0.60	0.42	1.12
24	0.23	1.40	0.35	0.65	1.12
50	0.26	1.24	0.43	0.57	1.15
75	0.35	1.23	0.38	0.62	1.13
125	0.32	0.97	0.40	0.60	1.13
175	0.29	0.80	0.38	0.62	1.11
200	0.30	0.75	0.30	0.70	1.07
HSA + (SDS)/mM					
0	0.06	0.96	0.90	0.10	1.13
8	0.08	1.13	0.82	0.18	1.14
16	0.14	1.22	0.44	0.56	1.07
24	0.19	1.32	0.31	0.69	1.13
40	0.18	1.30	0.46	0.54	1.12
100	0.22	1.10	0.50	0.50	1.07
120	0.23	0.95	0.48	0.52	1.09
160	0.20	0.89	0.40	0.60	1.17
200	0.21	0.75	0.33	0.67	1.18

time indicates that in the presence of the protein–surfactant aggregates, the normal species resides in a microenvironment which is essentially devoid of water. Notably, the fractional contribution of the normal form decreases from 0.91 to 0.60 upon addition of 8 mM SDS to 10 μM BSA, as the tautomer emission is decreased and the ground state of the cation is stabilized as discussed already. The cation lifetime increases till a SDS concentration of 75 mM and decreases subsequently, due to the formation of free micelles and incorporation of the fluorophore therein, leading to an increased ESPT and consequently, faster depopulation of C*. The changes in the temporal parameter occur at higher SDS concentrations in presence of 10 μM HSA, thereby confirming a greater apparent CMC in this case.

The changes in the decay profiles of the tautomer emission ($\lambda_{em} = 455$ nm) are less prominent, as is expected, as the extent and not dynamics of ESPT is expected to be affected by the protein–surfactant interaction. However, the decays are observed to become faster upon addition of the proteins to the 2PBI/ SDS solution (Fig. S3). The rise time is 900 ps at all concentrations of the protein. A component of 4 ns, characteristic of the T* emission, is also present in all the decays. However, with the increase of the protein concentration, an additional component of 900 ps is observed. As this is the characteristic lifetime of C*, we assign it to the tail of the C* emission, which becomes progressively more intense upon addition of the proteins.

In heterogeneous systems like these, global compartmental analysis is an ideal method to extract the time constants and pre-exponential factors [25,26]. However, we have not used this analysis as the lifetimes of the normal, cationic and tautomeric are well characterized [1]. In our earlier studies [2–4], we have obtained the values of lifetimes to be remarkably similar to those obtained by Rodriguez-Prieto and coworkers. So, we have retained a similar mode of data analysis, for the sake of an easy comparison with the situation in SDS micelles, as the main theme of the present communication is to explore whether or not ESPT is affected by a disruption of the negatively charged interface between water and the surfactants.

4. Conclusion

The ratio of the quantum yield of tautomer to normal band of 2PBI is found to indicate the different extents of aggregation of SDS molecules with BSA and HSA. The decrease in the tautomer emission with increasing amount of protein is due to the increasing hydrophobicity in the Stern layer due to the formation of necklace and bead structure where the protein chain wraps around the micellar headgroups. These inferences from the steady state data are bolstered by the temporal features. The shift in the equilibrium between the normal and the cationic forms is reflected in the changed amplitudes of the decay components of their fluorescence. In summary, the present study has revealed that 2PBI is a potentially good probe to study the protein–surfactant interaction and similar macromolecular interactions.

Acknowledgement

This work has been supported by CSIR research grant no. 01 (1851)/03/EMR-II. TKM thanks UGC for a Senior Research Fellowship. The authors thank Dr. P.K. Gupta and Dr. K. Das of Biomedical Applications Section, Raja Ramanna Centre for Advanced Technology, Indore, for the time resolved fluorescence experiments.

Appendix A. Supplementary data

Supplementary data associated with this article can be found, in the online version, at doi:10.1016/j.cplett.2007.03.014.

References

[1] F. Rodriguez-Prieto, M. Mosquera, M. Novo, J. Phys. Chem. 94 (1990) 853.
[2] T.K. Mukherjee, P. Ahuja, A.L. Koner, A. Datta, J. Phys. Chem. B 109 (2005) 12567.
[3] T.K. Mukherjee, D. Panda, A. Datta, J. Phys. Chem. B 109 (2005) 18895.
[4] T.K. Mukherjee, A. Datta, J. Phys. Chem. B 110 (2006) 2611.
[5] X.H. Guo, N.M. Zhao, S.H. Chen, J. Teixeira, Biopolymers 29 (1990) 335.
[6] K. Takeda, H. Sasaoka, K. Sasa, H. Hirai, K. Hachiya, Y. Mariyama, J. Colloid Interf. Sci. 154 (1992) 385.
[7] A. Valstar, M. Almgren, W. Brown, M. Vasilescu, Langmuir 16 (2000) 922.
[8] N.J. Turro, X.-G. Lei, K.P. Ananthapadmanabhan, M. Aronson, Langmuir 11 (1995) 2525.
[9] P. Dutta, A. Halder, S. Mukherjee, P. Sen, S. Sen, K. Bhattacharyya, Langmuir 18 (2002) 7867.
[10] R. Das, D. Guha, S. Mitra, S. Kar, S. Lahiri, S. Mukherjee, J. Phys. Chem. A 101 (1997) 4042.
[11] A. Chakraborty, D. Seth, P. Setua, N. Sarkar, J. Phys. Chem. B 110 (2006) 16607.
[12] M. Vasilescu, D. Angelescu, M. Almgren, A. Valstar, Langmuir 15 (1999) 2635.
[13] Y. Moriyama, K. Takeda, Langmuir 15 (1999) 2003.
[14] X.M. He, D.C. Carter, Nature 358 (1992) 209.
[15] J. Steinhardt, J. Krijn, J.G. Leidy, Biochemistry 10 (1971) 4005.
[16] C. La Mesa, J. Colloid Interf. Sci. 286 (2005) 148.
[17] P. Hazra, D. Chakrabarty, A. Chakraborty, N. Sarkar, Biochem. Biophys. Res. Commun. 314 (2004) 543.
[18] Y. Moriyama, D. Ohta, K. Hachiya, Y. Mitsui, K. Takeda, J. Protein Chem. 15 (1996) 265.
[19] K. Das, B. Jain, H.S. Patel, J. Phys. Chem. A 110 (2006) 1698.
[20] E.L. Gelamo, M. Tabak, Spectrochim. Acta A 56 (2000) 2255.
[21] C.A. Bonton, F. Nome, F.H. Quina, L.S. Romsted, Accounts Chem. Res. 24 (1991) 357.
[22] M.S. Fernandez, P. Fromherz, J. Phys. Chem. 81 (1977) 1755.
[23] D. Roy, R. Karmakar, S.K. Mondal, K. Sahu, K. Bhattacharyya, Chem. Phys. Lett. 399 (2004) 147.
[24] K. Sahu, D. Roy, S.K. Mondal, R. Karmakar, K. Bhattacharyya, Chem. Phys. Lett. 404 (2005) 341.
[25] L.V. Dommelen, N. Boens, F.C. De Schryver, M. Ameloot, J. Phys. Chem. 99 (1995) 8959.
[26] N. Boens, F.C. De Schryver, Chem. Phys. 325 (2006) 461.